ILASS 2008
Sep. 8-10, 2008, Como Lake, Italy

Paper ID ILASS08-13-4

SPRAY IMPINGEMENT MODEL BASED ON THE METHOD OF MOMENTS

D. P. Jones and A. P. Watkins *
School of Mechanical, Aerospace and Civil Engineering
The University of Manchester, Manchester, UK, M60 1QD

ABSTRACT

This paper deals with revisions and extensions to the spray model presented by Beck [1]. The model transports three sets of three consecutive moments of the underlying droplet size distribution in order to simulate injection and wall impaction. The underlying distribution is assumed to be of the form of a Gamma distribution [2]. A weak relation is assumed between the droplet velocity and its size. This relation is used to re-cast the collision and inter-phase drag models. Wet and dry wall conditions are considered, along with transportation of rebounding and splashing droplets. Higher order differencing schemes are assessed and details on the implementation of the model are given.

INTRODUCTION

Beck [1] presented a poly-disperse spray model which relied only on the knowledge of two local moments of its distribution, the total surface area and total volume per unit volume, μ_2 and μ_3. This model was later extended to account for the general effect on the spray upon impingement with a wall [3]. Both of these works focused on the physical representation of the spray, meanwhile using the simplest differencing schemes for the discretization of the transport equations.

The closure method was revised by assuming that the underlying distribution is of the form of a Gamma distribution [2]. This required the transportation of an additional moment to determine its two free parameters. To further this work, the Beta distribution was also tested [4] as another possible means of closure, which required the additional transportation of a fourth moment. However, the revisions had associated stability issues. In both cases, the additional transported moment was of a lower order than the lowest moment currently transported. The relatively quicker decay of lower order moments compared to μ_3 and the need to calculate moments of a couple of orders lower than the lowest transported moment resulted in inaccurate calculation of source terms relating to the moments and their momentum. In order to address the problems relating to the lower order moments, the current model is generalized such that any three consecutive moments can be transported.

The model is implemented in a new code, based on current numerical methods [5], so as to make use of higher order differencing schemes and enable improved resolution of the injector by using an unstructured grid topology.

Implementation of the wall impaction model is conceptually very simple. Boundary conditions relating to injected, rebounding and splashing droplets are assigned a unique set of moments respectively which interact with the gas phase. This method however, requires a large number of transport equations to be solved.

*Corresponding author: paul.watkins@manchester.ac.uk

METHOD

Moments

Assuming that the Probability Density Function (PDF) $\phi(r)$ and the total number of droplets μ_0 within a given volume is somehow known, moments of the droplet size distribution can be determined by

$$\mu_\alpha = \mu_0 \int_r \phi(r) r^\alpha \mathrm{d}r. \tag{1}$$

A number of methods are available for prescribing the general form of the PDF, such as assuming an a-priori form [2, 6], using polynomial fitting [6, 7] or the Maximum Entropy Formalism [8]. Whichever method is used, the specific form is determined though knowledge of the moments.

Presently, the Gamma distribution is used to determine the PDF. More advanced methods have been tested extensively [6, 7], however these require knowledge of consecutive moments from μ_0, which to date has not been implemented in the model successfully.

The Gamma distribution (Eq. 2) has two free parameters, k and θ and is capable of representing unimodal distributions with positive skew.

$$\phi(r) = \frac{r^{k-1}}{\Gamma(k)\theta^k} \exp\left(-\frac{r}{\theta}\right) \tag{2}$$

The two free parameters relate to the moments by

$$\frac{\mu_{j+1}}{\mu_j} = \theta(k+j). \tag{3}$$

From Eq. (3), the parameters can be related to three consecutive moments by

$$k = \frac{j\left(1+\frac{\mu_{j+2}\mu_j}{\mu_{j+1}^2}\right)+1}{\frac{\mu_{j+2}\mu_j}{\mu_{j+1}^2}-1} \quad (4)$$

$$\theta = \frac{\mu_{j+1}}{\mu_j(k+j)}. \quad (5)$$

It is important to note here that there is no guarantee that the denominator in the equation for k will be unconditionally positive since the transportation of the moments is not bounded in any way. In practice, a minimum value of 2.5 is set for k. The index j of the lowest order moment is currently set as 3.

Once the parameters are determined, moments of the Gamma distribution can be calculated by

$$\mu_\alpha|_{r_{lb}}^{r_{ub}} = \mu_0\, \theta^\alpha \frac{\Gamma(k+\alpha)}{\Gamma(k)} \left[\gamma\left(k+\alpha, \frac{r_{ub}}{\theta}\right) - \gamma\left(k+\alpha, \frac{r_{lb}}{\theta}\right)\right], \quad (6)$$

where r_{lb} and r_{ub} indicate the lower and upper limits of the integral and $\gamma(k, x)$ is the lower incomplete Gamma function.

Moment-Averaging

A moment-averaged quantity Ψ_α is obtained from the PDF and the variation of the quantity with respect to the droplet radius $\psi(r)$ by

$$\Psi_\alpha = \frac{\int_r \phi(r)\, r^\alpha\, \psi(r)\mathrm{d}r}{\int_r \phi(r)\, r^\alpha \mathrm{d}r}. \quad (7)$$

Beck assumed that the droplet velocity had no relation to the droplet radius. The current approach is to assume a weak relation based on the condition that in the limit of zero drop size the droplet is travelling at the continuum phase velocity $\vec{v}$, which gives

$$\vec{v}_{d,\alpha}(r) = \vec{v} + \vec{\delta}_\alpha r^\beta, \quad (8)$$

where ($\beta \simeq 0.1$). Combining the above two equations, the coefficient in Eq. (8) can be found as a function of the moment-averaged velocity,

$$\vec{\delta}_\alpha = \left(\vec{V}_{d,\alpha} - \vec{v}\right)\frac{\mu_\alpha}{\mu_{\alpha+\beta}}. \quad (9)$$

This velocity-radius relation can now be made use of when deriving the source terms of the spray transport equations.

Transport Equations

The conservation of moments (Eq. 10) is analogous to the mass conservation of the continuum phase.

$$\frac{\partial}{\partial t}\int_\Omega \mu_i \mathrm{d}\Omega + \int_S \vec{V}_{d,i}\cdot\vec{n}\mu_i \mathrm{d}S = \int_\Omega q_{\mu_i}\mathrm{d}\Omega. \quad (10)$$

The equation is discretized and solved like a typical scalar transport equation with the exception that the flux summation term within the main coefficient is retained.

The moment-averaged momentum transport equations (Eq. 11) have their respective moments as coefficients in the temporal and convection terms. Since a given set of moments represent a single distribution, the entire set of moments must be present to represent droplets in a given region. The momentum equation is described in terms of the total derivative to emphasize that the terms normally cancelled from its expansion must be retained for this equation since the coefficient μ_i is not constant.

$$\frac{D}{Dt}\int_\Omega \mu_i \vec{V}_{d,i}\mathrm{d}\Omega = \int_\Omega q_{\vec{V}_{d,i}}\mathrm{d}\Omega. \quad (11)$$

Source Terms

Inter-phase drag, droplet break-up and inter-droplet collisions contribute to the source terms of the above transport equations. Here only the inter-phase drag will be detailed as an example of the incorporation of the new droplet velocity definition. The drag force acting on a single droplet is given by

$$\vec{F}_{dr} = \frac{1}{2}C_d\rho A_d \parallel \vec{v} - \vec{v}_d(r) \parallel (\vec{v} - \vec{v}_d(r)). \quad (12)$$

Dividing though by droplet mass and integrating over all droplets according to the power of the associated moment-averaged velocity gives

$$\frac{\mathrm{d}\vec{V}_{d,i}}{\mathrm{d}t} = \frac{3}{8}\frac{\rho}{\rho_d}\mu_0 \int_r \frac{C_d}{r} \parallel \vec{v} - \vec{v}_{d,i}(r) \parallel (\vec{v} - \vec{v}_{d,i}(r))\ \phi(r) r^i \mathrm{d}r, \quad (13)$$

where the drag coefficient is defined as

$$C_d = \begin{cases} 4.093 & \text{if } Re_{d,i} \le 10 \\ 24Re_{d,i}^{-1} + 3.48Re_{d,i}^{-0.313} & \text{if } 10 < Re_{d,i} \le 1000 \\ 0.424 & \text{if } Re_{d,i} > 1000, \end{cases} \quad (14)$$

where $Re_{d,i}$ is the droplet Reynolds number based on the difference between i^{th} moment-averaged velocity and the gas phase velocity. The conditions relating to the drag coefficient are rearranged to provide critical radii, $r_{a,i}$ and $r_{b,i}$ respectively. The source term is then made up of three parts: the integral of Eq. (13) between 0 and $r_{a,i}$, $r_{a,i}$ and $r_{b,i}$ and lastly between $r_{b,i}$ and ∞. The final form of the source is

$$\begin{aligned} q_{\vec{V}_{d,i}} = \frac{\vec{\delta}_i}{\rho_d}(&1.534\rho \parallel \vec{\delta}_i \parallel \mu_{i-1+2\beta}|_0^{r_{a,i}} \\ &+ 4.5\mu\, \mu_{i-2+\beta}|_{r_{a,i}}^{r_{b,i}} \\ &+ 1.05\mu^{0.313}\left(\rho \parallel \vec{\delta}_i \parallel\right)^{0.687} \mu_{i-1.313+1.687\beta}|_{r_{a,i}}^{r_{b,i}} \\ &+ 0.159\rho \parallel \vec{\delta}_i \parallel \mu_{i-1+2\beta}|_{r_{b,i}}^{\infty}). \end{aligned} \quad (15)$$

Boundary Conditions

Inlet conditions for the moments at the injector are determined by defining the size distribution, obtaining the required moments. The distribution is intended to imply primary break-up of the bulk liquid has already taken place.

Wall boundary conditions are based on the spray impingement model of Bai & Gosman [9], where condition of the wall and the state of the impinging spray determine the outcomes. If the wall is dry the velocity and moments of the splashing droplets are determined. If the wall is wet, rebounding conditions in addition to splashing conditions are defined. For dry walls, splashing takes place when

$$We_d > C_{s1}La^{-0.18} \quad (16)$$

where C_{s1} is taken as 2634 and La is the Laplace number and We_d is the Weber number based on the velocity of μ_3. For wetted walls, rebound takes place when

$$We_d < 5 \tag{17}$$

and splashing when

$$We_d > C_{s2} La^{-0.18} \tag{18}$$

where C_{s2} is taken as 1320. Droplets outside these ranges are assumed to stick to the wall. From these conditions, critical radii are determined and then used to integrate over the near-wall droplet distribution, obtaining the appropriate boundary condition moments for the splashing and rebounding spray. The splashing process is assumed to double the number of droplets. The droplets which neither splash or rebound are assumed to stick. No consideration for spreading is taken at present. The sticking droplets are removed from the computational domain to prevent a build-up of liquid in the near-wall control volume. Corresponding droplet velocities are calculated from the volume-averaged incoming velocity and the wall normal vector.

$$\begin{aligned}
\vec{v}_{in} &= \vec{V}_{d,3} && (19)\\
\vec{v}_n &= (\vec{v}_{in} \cdot \vec{n})\, \vec{n} && (20)\\
\vec{v}_t &= \vec{v}_{in} - \vec{v}_n && (21)\\
\vec{v}_{out} &= -C_n \vec{v}_n + C_t \vec{v}_t && (22)
\end{aligned}$$

For rebounding droplets, the process is assumed to be inelastic, resulting in the coefficients taking

$$\begin{aligned}
C_n &= 0.993 - 1.76\theta + 1.56\theta^2 - 0.49\theta^3 && (23)\\
C_t &= 0.714 && (24)
\end{aligned}$$

where θ is the incidence angle. Splashing droplets take identical coefficients of 0.25 [3].

Differencing Schemes

To date, only first order schemes have been used for both the temporal and spatial differencing. Here, attempts at improving both schemes are presented. For temporal discretization, the Three Time Level method is adopted [5], which is a second order implicit scheme and has no time step constraint. For spatial discretization, the Total Variation Diminishing (TVD) method is implemented explicitly [10] for all transported properties and blended with the implicit Upwind differencing scheme. For the continuum, since it is entrained and accelarated by the spray interaction, the limiter ought to be based on the central differencing stencil such that the continuum upstream of the spray is significantly effected by its downstream accelaration. For this, the Min-Mod flux limiter is used. The spray however, ought only to require uptream information. Using only the Upwind scheme though, causes unphysical radial spread of the spray immediately downstream of the injector (Fig. 1).

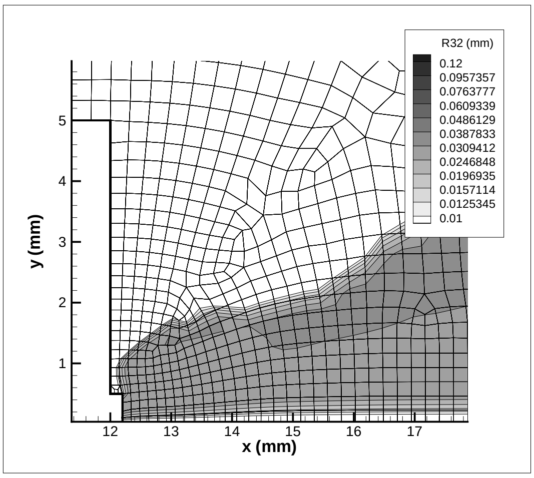

Figure 1: Unphysical radial spread infront of the injector using Upwind differencing.

This problem was overcome by Beck [1] by truncating the spray edge. Such an approach is possible on structured grids, but for general implementation, this method is not appropriate. Instead, the excessive diffusion is attempted to be reduced though the use of higher order differencing for face interpolation.

Once the injector is turned off, the Upwind scheme will cause rapid decay of trailing end of the spray. This would indicate that whichever higher order scheme is used, it must be capable of resolving both the progression of the spray and its decay, without exaggerating either. The only schemes suitable for this would be the Central Differencing scheme or TVD scheme using the Min-Mod limiter.

Implementation

The transportation of three sets of four moments and their corresponding velocities results in an additional 48 equations (in three dimensional space) to be solved along with the continuum phase equations. To minimise such a work load, the moments equation and the momentum equation are treated such that their arguments locally are a vector and matrix of variables respectively (Eqs. 25 and 26). Such approach provides local structure irrespective of the grid topology, allowing the Single Instruction, Multiple Data (SIMD) paradigm to be exploited.

$$\begin{aligned}
\mu_i &\rightarrow \underline{\mu} && (25)\\
\vec{V}_{d,i} &\rightarrow \underline{\vec{V}}_d \rightarrow \underline{\underline{V}}_d && (26)
\end{aligned}$$

Care must be taken in the setup of the coefficients for the momentum equation. It should not be assumed that if one moment has been transported to a given control volume, that all the other moments have also. It is recommended that the momentum coefficient μ_i is defined as

$$\mu_i = \begin{cases} \mu_i & \text{if } \mu_3 > C_\mu \text{ and } \mu_j > 0,\ \forall_j \\ 0 & \text{otherwise,} \end{cases} \tag{27}$$

where the cutoff C_μ is set to 10^{-7}. This condition is also necessary when calculating source terms and boundary conditions. In the case of calculating source terms, it has been found that a larger cutoff is required to maintain stability. This is set to 10^{-6}.

The implementation of the higher order differencing schemes for the momentum equation requires conditioning so as to turn off the higher order scheme at the spray edge. This is done by setting the blending constant γ to zero at any given interior face if either the pole coefficient $\mu_{i,\mathrm{P}}$ or neighbour coefficient $\mu_{i,\mathrm{N}}$ about that face is not greater than zero.

To ensure numerically sensible numbers for the moments, it is recommended that length base unit is scaled. Whilst such a practice is not essential for closure based on a-priori distributions, it is necessary when using more advanced closure methods.

Finally, when the injector is being switched on and off, a smooth profile is employed to gradually increase and decrease the liquid volume fraction exiting the injector along with the injection velocity.

RESULTS

For assessing the current model, a sample case from the experiments of Park, et al [11] is modelled: the injection of Iso-Octane onto a flat plate normal to the injector, 38mm downstream of the nozzle at ambient chamber conditions, assuming wet impaction conditions. Although the gas phase is initially assumed to be stagnant, turbulent conditions are initialized based on the characteristic speed set as approximately equal to the maximum gas phase speed and a turbulent intensity of 5%. The characteristic length set as ten times the injector radius. The injector is turned off after 0.5ms, though the simulation is run for 5ms. The injector radius is divided over four control volumes (Fig. 1), whilst retaining aspect ratios of all volumes close to unity (Fig. 2).

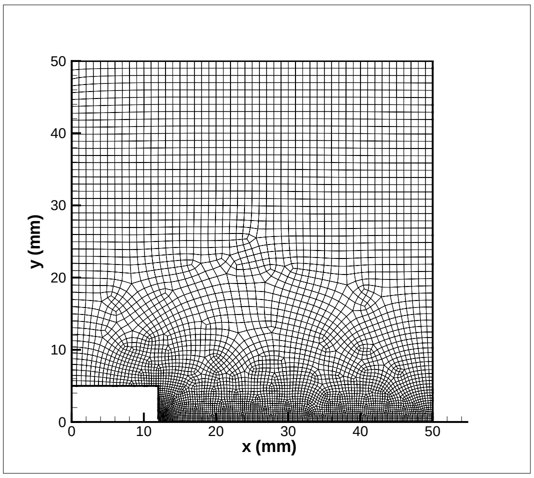

Figure 2: Computational domain.

Figures (3 – 9) show the liquid volume fraction of the spray rapidly decaying as the droplets move downstream. Exccess spread of the outer edge of the spray is shown, although the spray is very dilute in this region. Experimental results show a maximum spray thickness of approximately 16mm and a wetted footprint of diameter 22mm. Upon impingement, droplets are drawn both towards the centreline and outwards, tangential to the wall by the gas flow, resulting in a relatively small consentrated region and a large dilute region, respectively.

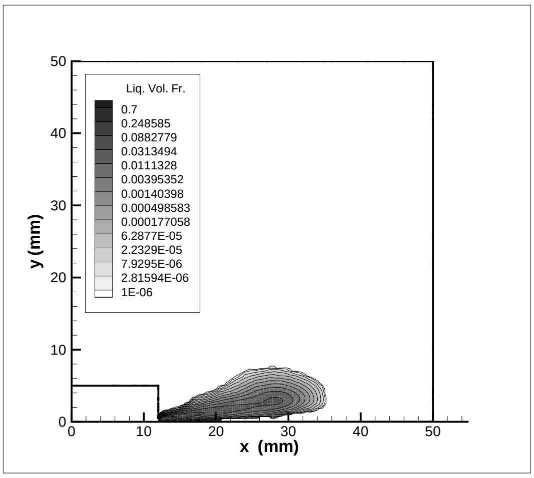

Figure 3: Liquid volume fraction of the spray after 0.25ms.

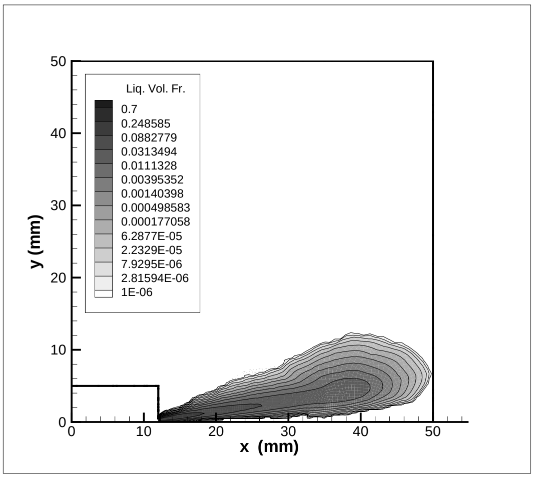

Figure 4: Liquid volume fraction of the spray after 0.5ms.

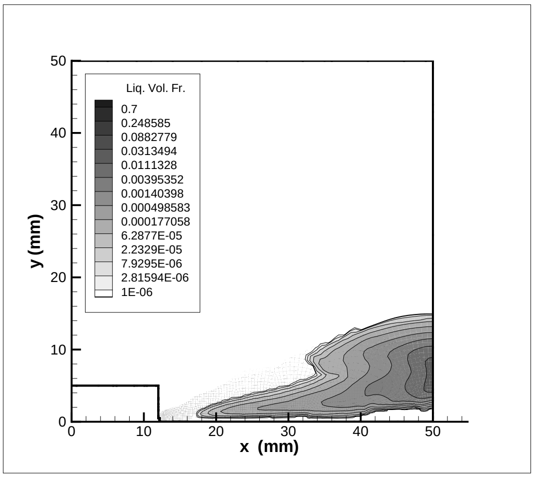

Figure 5: Liquid volume fraction of the spray after 1ms.

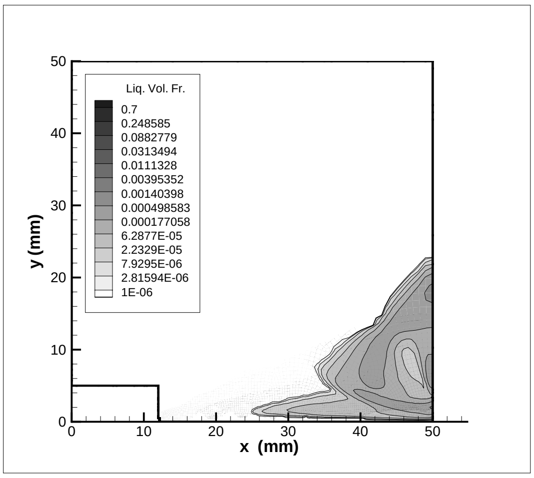

Figure 6: Liquid volume fraction of the spray after 2ms.

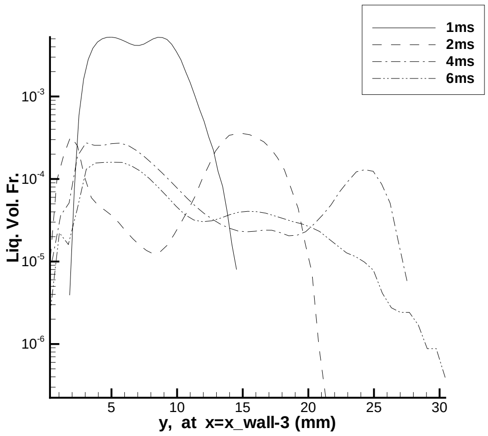

Figure 9: Liquid volume fraction at 3mm infront of the wall at different times.

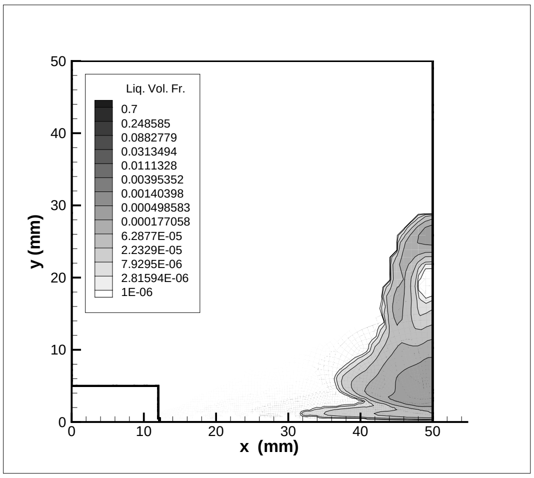

Figure 7: Liquid volume fraction of the spray after 4ms.

Sauter mean radius in Fig. (10 – 16) is shown to drop off at the back end of the spray once the injector is turned off, reflecting the greater relative effect of the drag force on the smaller droplets. As the spray impacts with the wall, the larger droplets at the front of the spray either stick or are broken up due to splashing, resulting in a much smaller mean droplet size. Due to the droplets generally being small after impaction, there is insufficient momentum to rebound the spray back into the body of the oncoming droplets and instead are dragged radially outwards by the primary vortex of the gas flow.

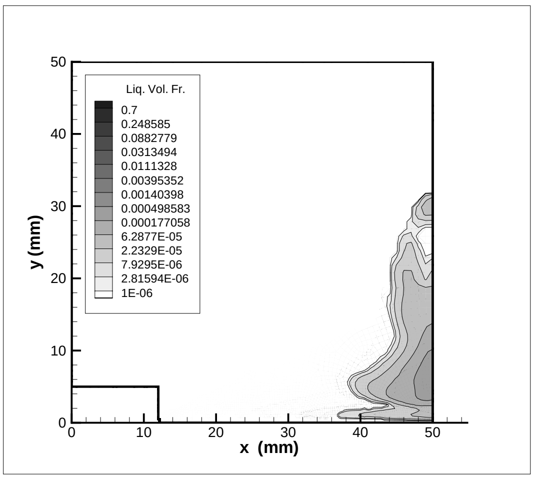

Figure 8: Liquid volume fraction of the spray after 6ms.

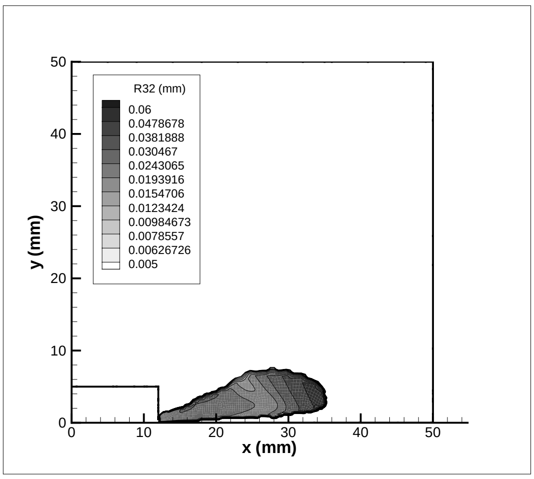

Figure 10: Sauter mean radius of the spray after 0.25ms.

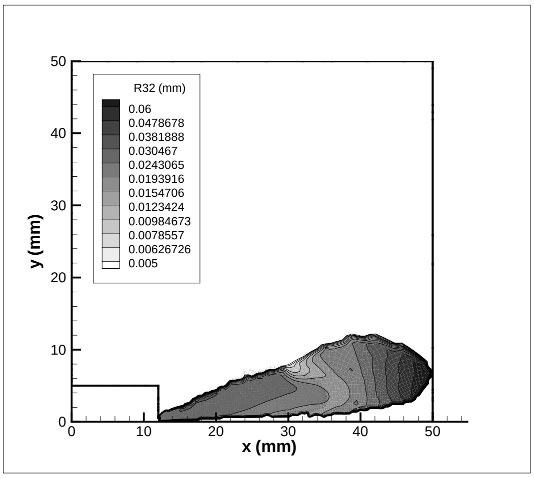

Figure 11: Sauter mean radius of the spray after 0.5ms.

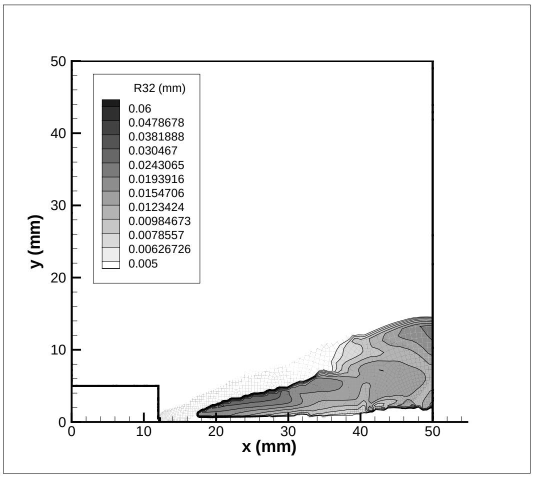

Figure 12: Sauter mean radius of the spray after 1ms.

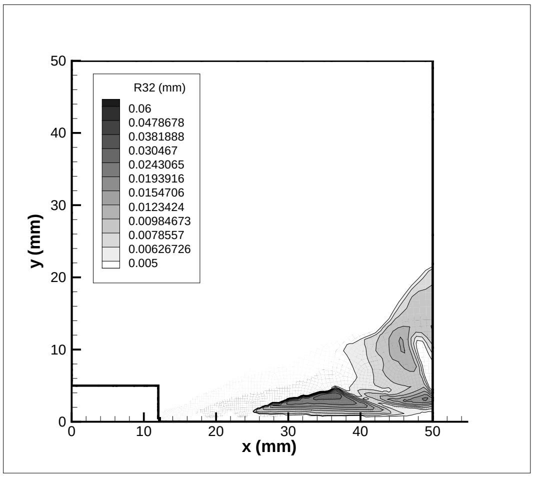

Figure 13: Sauter mean radius of the spray after 2ms.

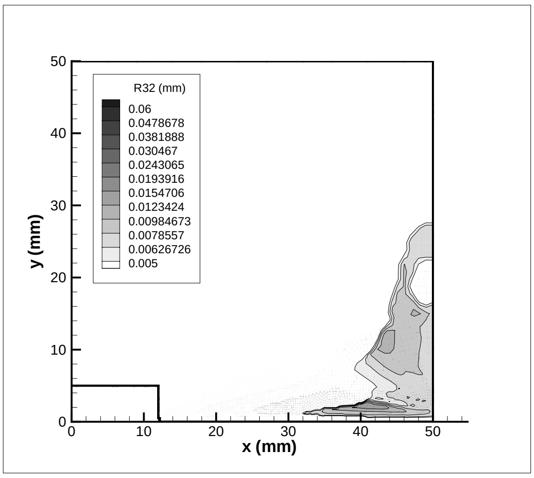

Figure 14: Sauter mean radius of the spray after 4ms.

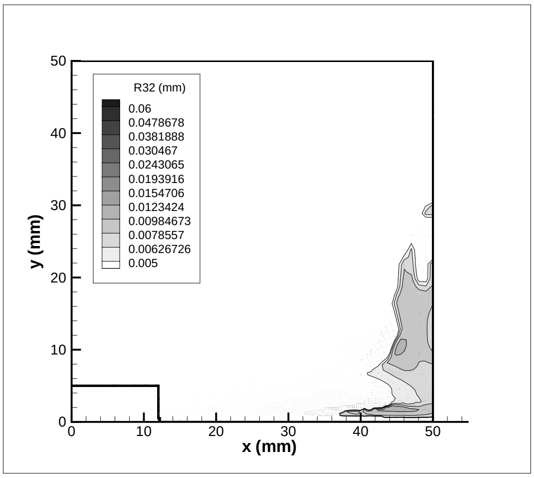

Figure 15: Sauter mean radius of the spray after 6ms.

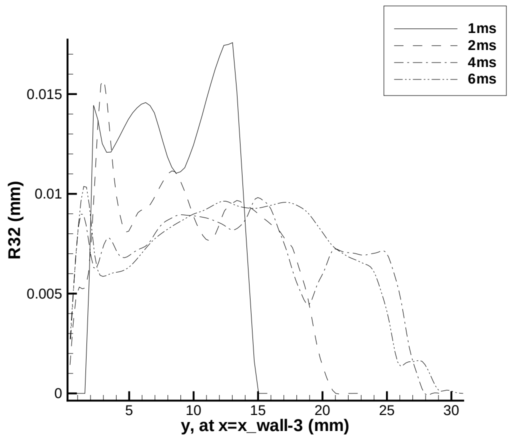

Figure 16: Sauter mean radius at 3mm infront of the wall at different times.

For this case the higher order blending was set at $\gamma = 0.2$ (i.e. 80% Upwind, 20% TVD: Min-Mod) for both the moments and their momentums. Increased blending was tested ($\gamma = 0.4,\ 0.7$), however the algorthm diverged shortly after 250 time steps (0.5ms) in both cases. As expected the increased blending does reduce the radial spread, as shown in the comparision between Fig. (1) and Fig. (17), presenting a more realistic profile.

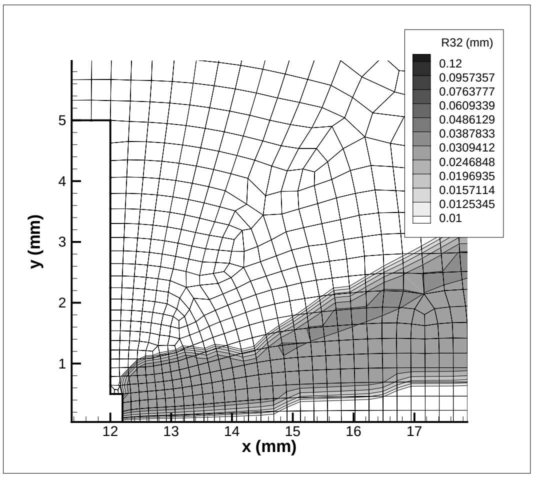

Figure 17: Radial spread with 30% Upwind, 70% TVD: Min-Mod.

CONCLUSIONS

The extension to the spray model has been implemented successfully, providing a sensible account of the spray behaviour upon impingement. Computational time required to solve the spray model is approximately equal to the time required to solve the continuous phase equations. The use of higher order convection schemes for the moments equation remains problematic and so further work is required in this area. Although averaged data is presented, it would be possible to recover the ensemble size distribution at any point in the spray, along with specific details relating to the injected, rebounding and splashing droplets.

NOMENCLATURE

A	Surface area, m^2
C	Constant
k	Gamma function argument
n	Normal
q	Source term
r	Droplet radius, m
S	Face area, m^2
t	Time, s
$\vec{V}, \vec{v}$	Velocity, $m\,s^{-1}$

Greek Symbols

γ	Spatial blending
$\Gamma(k)$	Gamma function
δ_i	Velocity-radius coefficient, $m^{1-\beta}\,s^{-1}$
θ	Angle, Gamma distibution parameter
μ	Viscosity, $kg\,m^{-1}\,s^{-1}$
μ_i	Moment, m^{i-3}
ρ	Density, $kg\,m^{-3}$
$\phi(r)$	Probability density function
Ψ	Moment-averaged quantity
$\psi(r)$	radius dependent quantity
Ω	Volume, m^3

Subscripts

c	Critical
d	Dispersed phase
i, j	Integer index
lb	Lower bound
N	Neighbour control volume
P	Pole control volume
ub	Upper bound
α	Real index

Superscripts

β	Velocity-radius exponent

REFERENCES

[1] J. C. Beck and A. P. Watkins. On the development of spray submodels based on droplet size moments. *J. of Comp. Phys.*, 182:586–621, 2002.

[2] B. Yue and A. P. Watkins. mathematical development and numerical analysis of further transport equations for the droplet size moment theory. *19th Annual Meeting of the Institute for Liquid Atomization and Spraying Systems (Europe)*, 2004.

[3] E. Lemini and A.P. Watkins. Development of a spray wall impaction model without discretisation into droplet size classes. *ILASS-Europe 2002*, 2002.

[4] A. P. Watkins. Transportation of sprays using the beta distribution. *20th Annual Meeting of the Institute for Liquid Atomization and Spraying Systems (Europe)*, 2005.

[5] J. H. Ferziger and M. Perić. *Computational Methods for Fluid Dynamics*. Springer, 3 edition, 2002.

[6] V. John, I. Angelov, A. A. Oncul, and D. Thevenin. Techniques for the reconstruction of a distribution from a finite number of its moments. *Chemical Engineering Science*, 62:2890–2904, 2007.

[7] G. Talenti. Recovering a function from a finite number of moments. *Inverse Problems*, 3:501–517, 1987.

[8] M. Ahmadi and R. W. Sellens. A simplified maximum-entropy-based drop size distribution. *Atomization and Sprays*, 3:291–310, 1993.

[9] C. Bai and A.D. Gosman. Development of methodology for spray impingement simulation. *SAE Technical Paper Series*, (950283), 1995.

[10] M.S. Darwish and F. Moukalled. Tvd schemes for unstructured grids. *Int. J. of Heat and Mass Transfer*, 46:599–611, 2003.

[11] J. S. Park, H. S. Kim, and M. C. Lai. Visualization and measurement of a narrow-cone di gasoline spray for the impingement analysis. *Int. J. of Automotive Technology*, 5(4):221–238, 2004.